also been predicted to extend into the FL regime (*46*). The study of magnetotransport in the DF will lead to further tests of hydrodynamics (*5*, *18*).

REFERENCES AND NOTES

1. L. P. Kadanoff, P. C. Martin, *Ann. Phys.* **24**, 419–469 (1963).
2. M. J. M. de Jong, L. W. Molenkamp, *Phys. Rev. B* **51**, 13389–13402 (1995).
3. C. Cao *et al.*, *Science* **331**, 58–61 (2011).
4. E. Shuryak, *Prog. Part. Nucl. Phys.* **53**, 273–303 (2004).
5. M. Müller, L. Fritz, S. Sachdev, *Phys. Rev. B* **78**, 115406 (2008).
6. M. Foster, I. Aleiner, *Phys. Rev. B* **79**, 085415 (2009).
7. S. S. Apostolov, A. Levchenko, A. V. Andreev, *Phys. Rev. B* **89**, 121104 (2014).
8. B. Narozhny, I. Gornyi, M. Titov, M. Schütt, A. Mirlin, *Phys. Rev. B* **91**, 035414 (2015).
9. K. S. Novoselov *et al.*, *Nature* **438**, 197–200 (2005).
10. Y. Zhang, Y. W. Tan, H. L. Stormer, P. Kim, *Nature* **438**, 201–204 (2005).
11. D. A. Siegel, W. Regan, A. V. Fedorov, A. Zettl, A. Lanzara, *Phys. Rev. Lett.* **110**, 146802 (2013).
12. D. E. Sheehy, J. Schmalian, *Phys. Rev. Lett.* **99**, 226803 (2007).
13. S. Sachdev, B. Keimer, *Phys. Today* **64**, 29 (2011).
14. C. H. Lui, K. F. Mak, J. Shan, T. F. Heinz, *Phys. Rev. Lett.* **105**, 127404 (2010).
15. M. Breusing, C. Ropers, T. Elsaesser, *Phys. Rev. Lett.* **102**, 086809 (2009).
16. K. J. Tielrooij *et al.*, *Nat. Phys.* **9**, 248–252 (2013).
17. J. C. Johannsen *et al.*, *Phys. Rev. Lett.* **111**, 027403 (2013).
18. S. A. Hartnoll, P. Kovtun, M. Müller, S. Sachdev, *Phys. Rev. B* **76**, 144502 (2007).
19. M. Müller, J. Schmalian, L. Fritz, *Phys. Rev. Lett.* **103**, 025301 (2009).
20. N. W. Ashcroft, N. D. Mermin, *Solid State Physics* (Brooks Cole, ed. 1, 1976).
21. Materials and methods are available as supplementary materials on *Science* Online.
22. N. Wakeham *et al.*, *Nat. Commun.* **2**, 396 (2011).
23. R. P. Smith *et al.*, *Nature* **455**, 1220–1223 (2008).
24. M. A. Tanatar, J. Paglione, C. Petrovic, L. Taillefer, *Science* **316**, 1320–1322 (2007).
25. R. W. Hill, C. Proust, L. Taillefer, P. Fournier, R. L. Greene, *Nature* **414**, 711–715 (2001).
26. L. Fritz, J. Schmalian, M. Müller, S. Sachdev, *Phys. Rev. B* **78**, 085416 (2008).
27. S. Adam, E. H. Hwang, V. M. Galitski, S. Das Sarma, *Proc. Natl. Acad. Sci. U.S.A.* **104**, 18392–18397 (2007).
28. J. Martin *et al.*, *Nat. Phys.* **4**, 144–148 (2008).
29. Y. Zhang, V. W. Brar, C. Girit, A. Zettl, M. F. Crommie, *Nat. Phys.* **5**, 722–726 (2009).
30. J. Xue *et al.*, *Nat. Mater.* **10**, 282–285 (2011).
31. C. R. Dean *et al.*, *Nat. Nanotechnol.* **5**, 722–726 (2010).
32. K. C. Fong, K. C. Schwab, *Phys. Rev. X* **2**, 031006 (2012).
33. L. Wang *et al.*, *Science* **342**, 614–617 (2013).
34. N. J. G. Couto *et al.*, *Phys. Rev. X* **4**, 041019 (2014).
35. J. Crossno, X. Liu, T. A. Ohki, P. Kim, K. C. Fong, *Appl. Phys. Lett.* **106**, 023121 (2015).
36. K. C. Fong *et al.*, *Phys. Rev. X* **3**, 041008 (2013).
37. A. C. Betz *et al.*, *Phys. Rev. Lett.* **109**, 056805 (2012).
38. C. B. McKitterick, D. E. Prober, M. J. Rooks, *Phys. Rev. B* **93**, 075410 (2016).
39. S. Yiğen, A. R. Champagne, *Nano Lett.* **14**, 289–293 (2014).
40. A. Laitinen *et al.*, *Nano Lett.* **14**, 3009–3013 (2014).
41. A. Lucas, J. Crossno, K. C. Fong, P. Kim, S. Sachdev, *Phys. Rev. B* **93**, 075426 (2016).
42. H. Yoshino, K. Murata, *J. Phys. Soc. Jpn.* **84**, 024601 (2015).
43. F. Ghahari *et al.*, http://arxiv.org/abs/1601.05859 (2016).
44. A. Lucas, *New J. Phys.* **17**, 113007 (2015).
45. P. K. Kovtun, D. T. Son, A. O. Starinets, *Phys. Rev. Lett.* **94**, 111601 (2005).
46. A. Principi, G. Vignale, M. Carrega, M. Polini, http://arxiv.org/abs/1506.06030 (2015).

ACKNOWLEDGMENTS

We thank M. Foster, D. Efetov, and G.-H. Lee for helpful discussions. The major experimental work at Harvard University is supported by the U.S. Department of Energy (grant DE-SC0012260) and at Raytheon BBN Technologies by Internal Research and Development. J.C. acknowledges support from the Function Accelerated nanoMaterial Engineering (FAME) Center, sponsored by Semiconductor Research Corporation MARCO and Defense Advanced Research Projects Agency. K.W. is supported by Army Research Office (ARO) Multidisciplinary University Research Initiative (MURI) (grant W911NF-14-1-0247). J.K.S. is supported by ARO (grant W911NF-14-1-0638) and the Agency for Science, Technology and Research (A*STAR). P.K. acknowledges partial support from the Gordon and Betty Moore Foundation's EPiQS Initiative (grant GBMF4543) and the Nano Material Technology Development Program through the National Research Foundation of Korea (grant 2012M3A7B4049966). A.L. and S.S. are supported by the NSF under grant DMR-1360789, the Templeton Foundation, and MURI grant W911NF-14-1-0003 from ARO. Research at the Perimeter Institute for Theoretical Physics is supported by the Government of Canada through Industry Canada and by the Province of Ontario through the Ministry of Research and Innovation. K.W. and T.T. acknowledge support from the Elemental Strategy Initiative conducted by the Ministry of Education, Culture, Sports, Science and Technology, Japan. T.T. acknowledges support from a Grant-in-Aid for Scientific Research (grant 262480621) and a grant on Innovative Areas "Nano Informatics" (grant 25106006) from the Japan Society for the Promotion of Science. T.A.O. and K.C.F. acknowledge support from Raytheon BBN Technologies. This work was performed, in part, at the Center for Nanoscale Systems (CNS), a member of the National Nanotechnology Infrastructure Network, which is supported by the NSF under award no. ECS-0335765. CNS is part of Harvard University.

SUPPLEMENTARY MATERIALS

www.sciencemag.org/content/351/6277/1058/suppl/DC1
Materials and Methods
Figs. S1 to S8
Table S1
References (*47*–*59*)

16 July 2015; accepted 6 January 2016
Published online 11 February 2016
10.1126/science.aad0343

ELECTRON TRANSPORT

Evidence for hydrodynamic electron flow in $PdCoO_2$

Philip J. W. Moll,[1,2,3] Pallavi Kushwaha,[3] Nabhanila Nandi,[3] Burkhard Schmidt,[3] Andrew P. Mackenzie[3,4]*

Electron transport is conventionally determined by the momentum-relaxing scattering of electrons by the host solid and its excitations. Hydrodynamic fluid flow through channels, in contrast, is determined partly by the viscosity of the fluid, which is governed by momentum-conserving internal collisions. A long-standing question in the physics of solids has been whether the viscosity of the electron fluid plays an observable role in determining the resistance. We report experimental evidence that the resistance of restricted channels of the ultrapure two-dimensional metal palladium cobaltate ($PdCoO_2$) has a large viscous contribution. Comparison with theory allows an estimate of the electronic viscosity in the range between 6×10^{-3} kg m^{-1} s^{-1} and 3×10^{-4} kg m^{-1} s^{-1}, versus 1×10^{-3} kg m^{-1} s^{-1} for water at room temperature.

In a quantum fluid without an associated lattice, such as ^{3}He, the momentum of the fluid is conserved except where it interacts with the walls of a channel through which it is flowing. As the temperature decreases and the quasiparticle-quasiparticle mean free path ℓ within the fluid increases (because of the decrease of its quasiparticle scattering rate), interactions with the walls become more probable and the viscosity and flow resistance increase. This is intuitively at odds with the behavior seen for electrons moving in a crystalline lattice, whose flow resistance decreases as ℓ increases. The resolution of this apparent paradox is that coupling to the lattice and its excitations means that the large majority of collisions in the electron fluid (electron-impurity, normal electron-phonon, Umklapp electron-electron, and Umklapp electron-phonon) relax momentum, taking the fluid far from the hydrodynamic limit. At least some of these momentum-relaxing collisions are inevitable in any real material. Strictly speaking, momentum of the electron fluid can never be conserved, even in a bulk sample for which boundary scattering is negligible. However, this does not mean that the electronic viscosity plays no role in determining electrical resistance. A pragmatic benchmark is whether momentum-conserving processes are faster or slower than momentum-relaxing ones. If the electron fluid's momentum is relaxed slowly, it can be thought of as being quasi-conserved, and hydrodynamic signatures might be observable (*1*–*9*).

The search for hydrodynamic effects in electrons in solids has been given extra impetus by the introduction of the "holographic correspondence" to condensed matter physics (*10*). This technique introduced the concept of a minimum viscosity, argued to be applicable to strongly

[1]Laboratory for Solid State Physics, ETH Zürich, CH-8093 Zürich, Switzerland. [2]Department of Physics, University of California, Berkeley, CA 94720, USA. [3]Max Planck Institute for Chemical Physics of Solids, 01187 Dresden, Germany. [4]Scottish Universities Physics Alliance, School of Physics and Astronomy, University of St. Andrews, St. Andrews KY16 9SS, UK.
*Corresponding author. E-mail: andy.mackenzie@cpfs.mpg.de

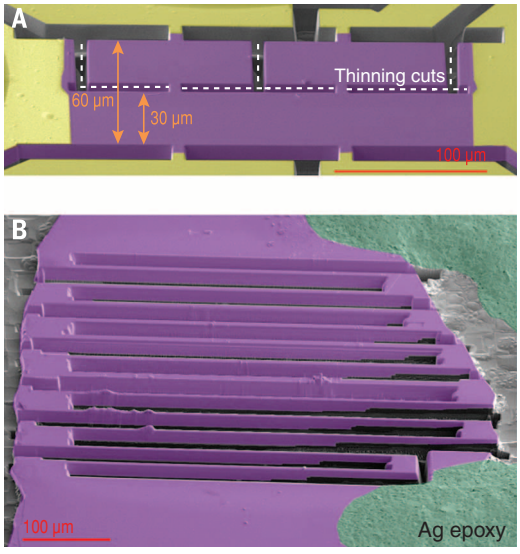

Fig. 1. FIB-prepared devices of $PdCoO_2$ crystals. (**A**) The crystal used for our channel-thinning experiment, after the first two processing steps. An initial channel 120 μm wide has been reprocessed to produce a narrower conducting channel of width 60 μm. The same channel was subsequently reprocessed seven further times, narrowing it by approximately half each time, until it was 0.7 μm wide. (**B**) A meander channel processed in a second crystal for use in a search for the Shubnikhov–de Haas effect. Its approximate width is 6 μm in the narrowed parts; thickness is 17 μm. Its resistance in a magnetic field of 14 T at a temperature of 2 K is 5.7×10^{-3} ohms.

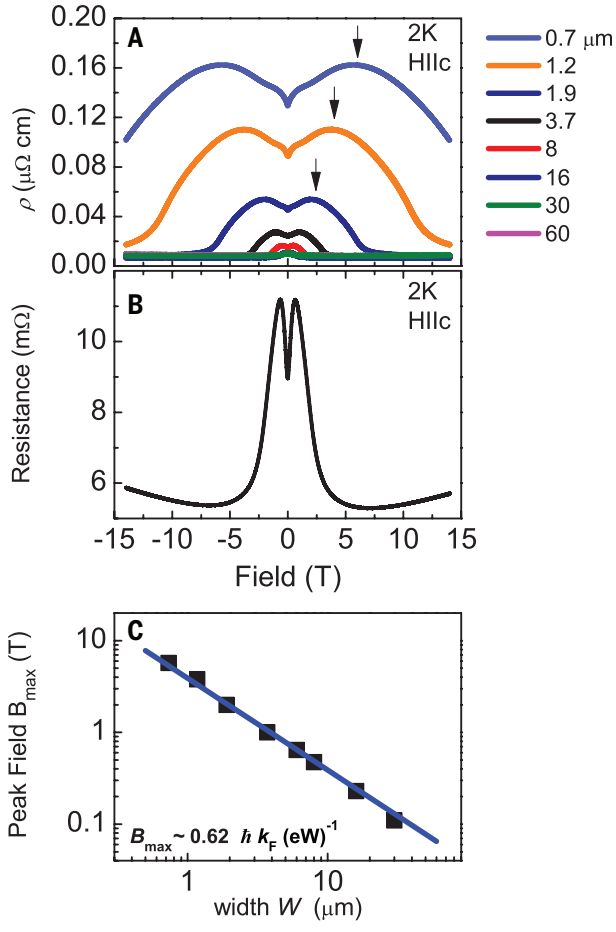

Fig. 2. Effect of channel width *W* on magnetotransport. (**A**) Magnetoresistance data from the sample shown in Fig. 1A taken at 2 K after successive channel-thinning steps. (**B**) Magnetoresistance data from the sample shown in Fig. 1B taken at 2 K. (**C**) B_{max} [indicated by arrows in (A)] varies as $\alpha(\hbar k_F/We)$ as the device shown in Fig. 1A is successively thinned. Both the functional form and prefactor are in good agreement with theory and with previous measurements on semiconductor wires.

interacting fluids as diverse as the quark-gluon plasma and cold atomic gases (*11*). Hydrodynamic effects have also been postulated to be at the root of the temperature-linear resistivity of the high-temperature superconductors (*6*, *7*), but because momentum-relaxing scattering is strong in those materials, it is difficult to perform an analysis of the experimental data that unambiguously separates the two effects. In a pioneering experiment, unusual current-voltage relationships in a semiconductor wire were convincingly ascribed to hydrodynamic effects (*3*), but that avenue of research has not been widely pursued, even though the large difference between transport and electron-electron scattering rates in semiconductors was later demonstrated by direct nonequilibrium measurements (*12*).

To investigate whether a hydrodynamic contribution to electrical transport can be clearly separated from the more standard contributions from momentum-relaxing processes, we sought a material in which momentum-relaxing scattering is anomalously suppressed. The material that we chose was $PdCoO_2$, a layered metal with a number of unusual properties (*13*–*21*). Its electronic structure is deceptively simple, with one highly dispersive band, dominantly of Pd 4d/5s character, crossing the Fermi level (*22*–*26*). Its Fermi volume corresponds to one electron per formula unit to high accuracy (*18*), and the ratio of in-plane to out-of-plane resistivity is approximately 10^3, justifying the use of a two-dimensional approximation in treating the in-plane properties.

The electrical conductivity of $PdCoO_2$ is remarkable. At room temperature, its resistivity is just 2.6×10^{-6} ohm·cm, 30% lower per carrier than that of elemental copper. Below 15 K, the resistivity is essentially independent of temperature; in the best single crystals, the resistivity is below 1×10^{-8} ohm·cm (*18*). This striking behavior might be attributable to phonon drag, in which the phonons follow the electrons into an out-of-equilibrium distribution when an electric field is applied. In $PdCoO_2$, the activation temperature for Umklapp electron-phonon processes is at least 160 K, unusually high for a metal (*18*).

These properties make $PdCoO_2$ a good candidate for a search for hydrodynamic effects. Below 15 K, momentum-relaxing processes are far slower than those observed in most metals. Better still, if phonon drag is indeed taking place, the normal electron-phonon processes that usually impede electrons in solids from approaching the hydrodynamic limit are now helping that process instead, because they contribute a source of momentum-conserving scattering. An important independent hint that the balance between momentum-conserving and momentum-relaxing scattering is both unusual and favorable for the observation of hydrodynamic effects comes from the ratio of the mean free paths deduced, respectively, from the resistivity, which is sensitive to processes that efficiently relax momentum, and from analysis of the de Haas–van Alphen (dHvA) effect, whose amplitude is sensitive to a wider range of scattering processes. The inverse of that ratio is 5 to 10%, an unusually small value approximately an order of magnitude lower than that seen in ordinary metals (*18*).

In a purely hydrodynamic fluid, flow resistance in channels is determined entirely by momentum-relaxing boundary scattering, the efficiency of which is determined by the fluid's viscosity. Boundary scattering also contributes to the resistance in thin wires or channels of metals in which hydrodynamic effects play no observable role, but the standard theory of this phenomenon is well established (*27*). We therefore set out to construct a series of $PdCoO_2$ "wires," study how their resistance varied with the channel width, and investigate whether there were observable deviations

from the predictions of standard theory. The wires were produced from flux-grown single crystals by focused ion beam (FIB) etching (Fig. 1A). Six such devices were made and shown to have consistent properties (*28*). We discuss the nature of the boundaries produced by FIB processing in (*28*) and show that damage is restricted to approximately 20 nm from the edge of the channel. Taking all uncertainties into account, the undamaged channel width can be determined to an accuracy of ±80 nm. For the main experiment, measurements were done on a single successively etched wire from the same crystal, to remove as many experimental uncertainties as possible. A second crystal (Fig. 1B) was etched into a meander channel ideally suited for a measurement of the Shubnikhov–de Haas (SdH) effect. For each experiment, we studied the magnetoresistance of the wire in magnetic fields B ranging from −14 T to +14 T. We also fabricated a multicontact device to verify that our data are length-independent at constant width (*28*).

Data obtained in the channel-narrowing experiment are shown in Fig. 2A for widths ranging from 60 μm to 0.7 μm at a measurement temperature of 2 K. Data from the meander channel are shown in Fig. 2B. Consistent with previous measurements on other single crystals (*18*), the resistivity in zero field for the 60-μm sample is 9×10^{-9} ohm·cm. The value of the momentum-relaxing mean free path ℓ_{MR} is a crucial parameter in the analysis of the resistance of restricted channels; the single-band electronic structure and well-known Fermi surface shape and volume (*16*, *18*) allow an accurate calculation of ℓ_{MR} = 18.5 + 1.5 μm (*28*). The wire widths W used for the experiment therefore cover the range $0.3 \leq \ell_{MR}/W \leq 26$, enabling study of the crossover between a nearly bulk regime and one in which a sample dimension falls far below the bulk mean free path.

We adopt the usual solid-state physics convention of describing the transport properties of our channels in terms of the resistivity ρ. For a channel of width W, length L, thickness T, and resistance R, $\rho \equiv RTW/L$. Conceptually, ρ is a bulk property of the material, so in the absence of boundary effects it should be independent of W. In contrast, at low fields, the overall channel resistivity ρ increases by more than an order of magnitude as the wire width is decreased (Fig. 2). Because this involves repeated exposure to ion beam etching, it is natural to wonder whether this trend is caused by beam damage increasing the scattering in the bulk of the wire. However, extending the data to higher fields proves that this is not the case. First, we note that at high fields, the resistivity is similar at all widths above 0.7 μm. Second, the pronounced maximum seen at fields B_{max} in the magnetoresistance for $W \leq$ 30 μm is a well-known phenomenon from the study of narrow conducting channels for which the bulk mean free path is on the order of the channel width or larger (*29*–*31*). For each channel width, the rise in the magnetoresistivity at low fields is stopped when the cyclotron orbit radius falls to less than the channel width, because the helical pitch of the motion of the drifting electrons becomes so tight that boundary scattering is suppressed, and eventually the bulk, width-independent resistivity is recovered at high fields. Specifically, $B_{max} = \alpha(\hbar k_F/We)$ (where $\hbar$ is Planck's constant divided by 2π, k_F is the Fermi wave vector, and e is the electronic charge) with constant $\alpha = 0.55$ has been reported for restricted channels of two-dimensional electron gas (*30*), and a similar functional form with α = 0.9 was observed in recent work on graphene (*31*). The data shown in Fig. 2C therefore provide further evidence that the overall scale of the resistivity is increasing because of additional boundary scattering rather than additional bulk scattering. Very low field peaks in the magnetoresistance can still be seen in the 30-μm channel, providing further direct geometrical evidence that ℓ_{MR} is long. Further evidence that extremely high bulk purity is retained after ion beam etching comes from the data from the meander sample. Its B_{max} is consistent with the

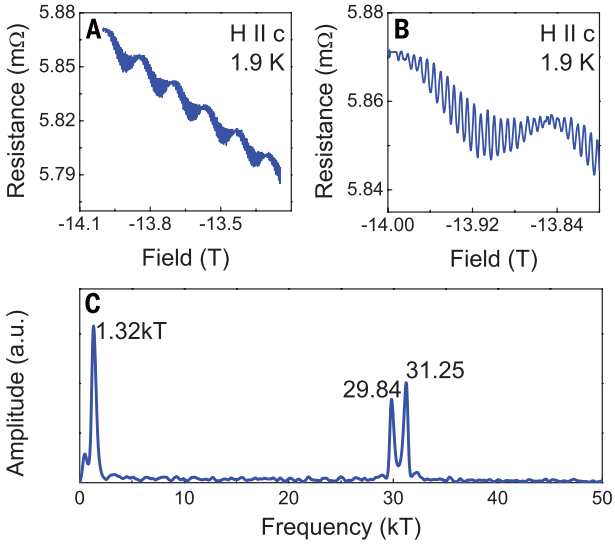

Fig. 3. Shubnikhov–de Haas oscillations. (**A** and **B**) SdH oscillations from the patterned meander track shown in Fig. 1B. (**C**) The frequencies of the SdH oscillations extracted by Fourier analysis of the data in (A).

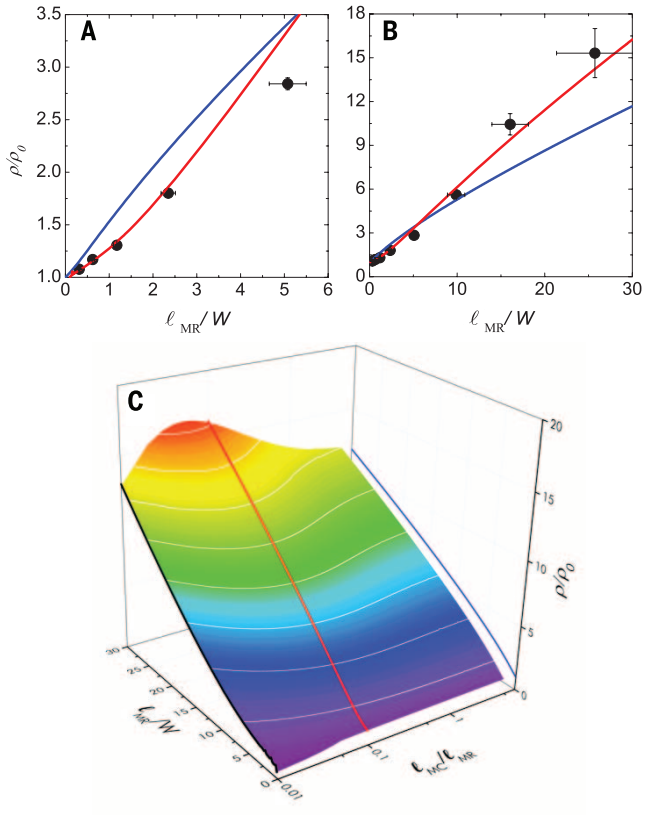

Fig. 4. Hydrodynamic effect on transport. (**A** and **B**) The measured resistivity of $PdCoO_2$ channels normalized to that of the widest channel (ρ_0), plotted against the inverse channel width $1/W$ multiplied by the bulk momentum-relaxing mean free path ℓ_{MR} (solid black circles). Blue solid line: Prediction of a standard Boltzmann theory including boundary scattering but neglecting momentum-conserving collisions. Red line: Prediction of a model that includes the effects of momentum-conserving scattering (see text). Error bars stem from uncertainties of sample dimension (*28*). (**C**) Predictions of the hydrodynamic theory over a wide range of parameter space.

measured width of 6 μm (Fig. 2, B and C), and at high fields, clear SdH oscillations are seen, with frequencies in agreement with those seen in dHvA oscillations from bulk crystals (*18*). High frequencies are particularly hard to see by the SdH effect; the 30-kT frequencies shown in Fig. 3B are among the highest ever reported in SdH measurements.

The data presented in Figs. 2 and 3 provide strong evidence that boundary rather than bulk scattering dominates the rise in resistivity seen as we reduce the channel width. As discussed above, boundary scattering is expected even in the absence of hydrodynamic effects as the channel width falls to less than the mean free path and the system enters the ballistic transport regime. The relevant theory (*4*, *27*) can be expressed in a useful dimensionless form, shown as a blue line in Fig. 4. If ρ is normalized to the bulk resistivity ρ_0 of an infinitely wide sample and plotted against ℓ_{MR}/W, the prediction has no free parameters. At $\ell_{MR}/W = 25$, ρ is calculated to be 10.3 ρ_0. Our measured value for ρ/ρ_0 is more than 50% larger than this prediction, and our data also show a functional form that is at odds with the simple theory.

To examine whether the large deviations of the data from the predictions of standard transport theory are linked to electronic hydrodynamics, we carefully studied the predictions of a more sophisticated theory that takes momentum-conserving scattering into account (*4*). Originally formulated to analyze the current-dependent hydrodynamic signatures reported in (*3*), the theory encodes momentum-relaxing scattering via the role of impurities and momentum-conserving scattering via normal electron-electron scattering processes. In $PdCoO_2$, the scale of momentum-conserving electron-electron scattering is uncertain because of Fermi surface faceting (*26*), and phonons dragged out of equilibrium are also likely to be making a contribution to the momentum-conserving processes. In this sense, even this more sophisticated theory is oversimplified, and it would be dangerous to use it to predict temperature-dependent transport in $PdCoO_2$. However, its results at any fixed temperature depend only on the ratio of a momentum-conserving mean free path ℓ_{MC} to the momentum-relaxing mean free path ℓ_{MR}, and the microscopic origin of the scattering that produced that ratio is not relevant. The theory is therefore a useful guide to the consequences of including hydrodynamic effects in experiments performed at constant temperature, such as the one shown in Fig. 4, A and B. For any value of ℓ_{MC}/ℓ_{MR}, it predicts a unique functional form and overall magnitude for ρ/ρ_0 versus ℓ_{MR}/W, with no free fitting parameters.

As can be seen from the red lines in Fig. 4, A and B, the hydrodynamic theory for $\ell_{MC}/\ell_{MR} = 0.1$ produces an excellent match to our data. In Fig. 4C we show how the predictions of the theory change as a function of ℓ_{MC}/ℓ_{MR}, marking the blue and red lines of Fig. 4, A and B, on the contour plot for reference. For large ℓ_{MC}/ℓ_{MR} (i.e., weak momentum-conserving scattering), it limits rapidly to the prediction of the standard theory. At its other limit of strong momentum-conserving scattering (black line), the prediction for ρ/ρ_0 is approximately quadratic as a function of ℓ_{MR}/W. In this regime, viscous effects dominate, and the W^{-2} dependence of ρ is equivalent to the W^{-3} prediction for flow resistance that is obtained from the purely hydrodynamic Navier-Stokes equation (*28*).

Our value for ℓ_{MC}/ℓ_{MR} (red line in Fig. 4C) sits between these limiting cases. Because viscosity is inversely proportional to ℓ_{MC}, the initial ~W^{-2} rise is steeper than for $\ell_{MC}/\ell_{MR} = 0.01$. As ℓ_{MR}/W rises toward 10, ℓ_{MC} is no longer much less than W, and the Navier-Stokes prediction evolves smoothly to a solution in which viscous effects are important but the channel constriction is such that we leave the purely hydrodynamic regime. Physically the system is in a hybrid situation in which traditional impurity and boundary scattering mix with viscosity-stimulated boundary scattering to produce the overall evolution of resistivity with channel width. Fig. 4C also shows that the hydrodynamic prediction is insensitive to the precise choice of ℓ_{MC}/ℓ_{MR}. Our choice of 0.1 was not the result of fitting, but simply an estimate motivated by the ratio of scattering rates deduced from measurements of resistivity and the dHvA effect. Choices that were larger or smaller by a factor of 2 would give a similar level of agreement with the data.

The data and predictions shown in Fig. 4 and discussed in (*28*) provide strong evidence that we have observed a substantial hydrodynamic contribution to electrical transport in a bulk material. Further analysis of the theory in its Navier-Stokes limit allows a quantitative estimate of the electronic viscosity itself as a function of the hydrodynamic contribution to ρ/ρ_0. As a result, we are able to estimate the dynamic viscosity η of the electronic fluid in $PdCoO_2$ as lying in the range between 6×10^{-3} kg m^{-1} s^{-1} and 3×10^{-4} kg m^{-1} s^{-1}. For comparison, the η values of two well-known fluids, water at room temperature and liquid nitrogen at 75 K, are 1×10^{-3} kg m^{-1} s^{-1} and 1×10^{-4} kg m^{-1} s^{-1}, respectively.

Although the bounds we can place on the electronic viscosity of $PdCoO_2$ are not very precise, we stress that this is an issue of theory, not experiment. We believe that there is such a large hydrodynamic contribution to our data that they contain all the information required to estimate the viscosity precisely, and we hope that our experiment motivates further work on this issue. As discussed above, $PdCoO_2$ is a weakly scattering system, so it is not surprising that a comparison of our estimate of η with measurements of the entropy density s (*15*, *18*) yields $\eta/s \approx 10^6\ \hbar/k_B$, far from a proposed minimum viscosity limit (*11*). It will also be interesting to reexamine a possible role of hydrodynamic effects in explaining the resistivity in systems in which the momentum-conserving scattering is extremely strong (*6*, *7*, *32*). In principle, a range of viscosities is to be expected in different electronic fluids, and even the attainment of turbulent electronic flow may be possible.

REFERENCES AND NOTES

1. R. N. Gurzhi, *Zh. Eksp. Teor. Fiz.* **44**, 771 (1963) [*Sov. Phys.* **17**, 521 (1963)].
2. R. N. Gurzhi, *Usp. Fiziol. Nauk* **94**, 689 (1968) [*Sov. Phys. Usp.* **11**, 255 (1968)].
3. L. W. Molenkamp, M. J. M. de Jong, *Phys. Rev. B* **49**, 5038–5041 (1994).
4. M. J. M. de Jong, L. W. Molenkamp, *Phys. Rev. B* **51**, 13389–13402 (1995).
5. B. Spivak, S. A. Kivelson, *Ann. Phys.* **321**, 2071–2115 (2006).
6. R. A. Davison, K. Schalm, J. Zaanen, *Phys. Rev. B* **89**, 245116 (2014).
7. S. A. Hartnoll, *Nat. Phys.* **11**, 54–61 (2015).
8. A. V. Andreev, S. A. Kivelson, B. Spivak, *Phys. Rev. Lett.* **106**, 256804 (2011).
9. R. Mahajan, M. Barkeshli, S. A. Hartnoll, *Phys. Rev. B* **88**, 125107 (2013).
10. S. A. Hartnoll, P. K. Kovtun, M. Müller, S. Sachdev, *Phys. Rev. B* **76**, 144502 (2007).
11. P. K. Kovtun, D. T. Son, A. O. Starinets, *Phys. Rev. Lett.* **94**, 111601 (2005).
12. C. P. Weber *et al.*, *Nature* **437**, 1330–1333 (2005).
13. R. D. Shannon, D. B. Rogers, C. T. Prewitt, *Inorg. Chem.* **10**, 713–718 (1971).
14. M. Hasegawa, I. Inagawa, M. Tanaka, I. Shirotani, H. Takei, *Solid State Commun.* **121**, 203–205 (2002).
15. H. Takatsu *et al.*, *J. Phys. Soc. Jpn.* **76**, 104701 (2007).
16. H.-J. Noh *et al.*, *Phys. Rev. Lett.* **102**, 256404 (2009).
17. H. Takatsu, S. Yonezawa, S. Fujimoto, Y. Maeno, *Phys. Rev. Lett.* **105**, 137201 (2010).
18. C. W. Hicks *et al.*, *Phys. Rev. Lett.* **109**, 116401 (2012).
19. H. Takatsu *et al.*, *Phys. Rev. Lett.* **111**, 056601 (2013).
20. R. Daou, R. Frésard, S. Hébert, A. Maignan, *Phys. Rev. B* **91**, 041113 (2015).
21. N. Kikugawa *et al.*, http://arxiv.org/abs/1412.5168 (2015).
22. M. Hasegawa *et al.*, *Mater. Trans.* **42**, 961–964 (2001).
23. V. Eyert, R. Frésard, A. Maignan, *Chem. Mater.* **20**, 2370–2373 (2008).
24. K. Kim, H. C. Choi, B. I. Min, *Phys. Rev. B* **80**, 035116 (2009).
25. K. P. Ong, J. Zhang, J. S. Tse, P. Wu, *Phys. Rev. B* **81**, 115120 (2010).
26. K. P. Ong, D. J. Singh, P. Wu, *Phys. Rev. Lett.* **104**, 176601 (2010).
27. C. W. J. Beenakker, H. van Houten, *Solid State Phys.* **44**, 1–228 (1991).
28. See supplementary materials on *Science* Online.
29. E. Ditlefsen, J. Lothe, *Philos. Mag.* **14**, 759–773 (1966).
30. T. J. Thornton, M. L. Roukes, A. Scherer, B. P. van de Gaag, *Phys. Rev. Lett.* **63**, 2128–2131 (1989).
31. S. Masubuchi *et al.*, *Phys. Rev. Lett.* **109**, 036601 (2012).
32. J. A. N. Bruin, H. Sakai, R. S. Perry, A. P. Mackenzie, *Science* **339**, 804–807 (2013).

ACKNOWLEDGMENTS

We thank J. C. Davis, C. Geibel, A. G. Green, S. A. Hartnoll, C. W. Hicks, S. A. Kivelson, Y. Maeno, T. Oka, J. W. Orenstein, and S. H. Simon for stimulating discussions and the UK Engineering and Physical Sciences Research Council for financial support. The FIB work was supported by the SCOPE-M center for electron microscopy at ETH Zürich. We thank P. Gasser, J. Reuteler, and B. Batlogg for FIB support. The data and/or materials supporting this publication can be accessed at http://dx.doi.org/10.17630/cdc6c488-2ea4-440e-a68d-e2a426709171.

SUPPLEMENTARY MATERIALS

www.sciencemag.org/content/351/6277/1061/suppl/DC1
Materials and Methods
Figs. S1 to S6
References (*33*–*39*)

24 June 2015; accepted 23 December 2015
Published online 11 February 2016
10.1126/science.aac8385

Science

Evidence for hydrodynamic electron flow in $PdCoO_2$

Philip J. W. Moll, Pallavi Kushwaha, Nabhanila Nandi, Burkhard Schmidt and Andrew P. Mackenzie

Science **351** (6277), 1061-1064.
DOI: 10.1126/science.aac8385originally published online February 11, 2016

Electrons that flow like a fluid

Electrons inside a conductor are often described as flowing in response to an electric field. This flow rarely resembles anything like the familiar flow of water through a pipe, but three groups describe counterexamples (see the Perspective by Zaanen). Moll *et al.* found that the viscosity of the electron fluid in thin wires of $PdCoO_2$ had a major effect on the flow, much like what happens in regular fluids. Bandurin *et al.* found evidence in graphene of electron whirlpools similar to those formed by viscous fluid flowing through a small opening. Finally, Crossno *et al.* observed a huge increase of thermal transport in graphene, a signature of so-called Dirac fluids.

Science, this issue p. 1061, 1055, 1058; see also p. 1026